On the XXX spin-1/2 quantum chain with non-diagonal boundary fields

Andreas Klümper and Xin Zhang

Abstract The XXX spin-$\frac{1}{2}$ Heisenberg chain with non-diagonal boundary fields is a cornerstone model in the study of integrable systems with open boundaries. Despite its significance, solving this model exactly poses significant challenges due to the breaking of $U(1)$ symmetry. Building on the off-diagonal Bethe Ansatz (ODBA), we analyze a set of non-linear integral equations (NLIEs) that characterize the exact spectrum of the model.

For $U(1)$-symmetric chains, the NLIEs involve two functions, $a(x)$ and $\bar{a}(x)$, coupled by short-range integration kernels. The solutions exhibit characteristic features at a length scale that grows logarithmically with the system size, N.

In the absence of $U(1)$ symmetry, a novel third function, $c(x)$, emerges to account for the additional term in the T-Q relation. This introduces long-range kernel elements, leading to a winding phenomenon in $\log(1+a(x))$ and $\log(1+\bar{a}(x))$, where these functions undergo a steep $2\pi\mathrm{i}$ increase at a characteristic scale x_1. Other features are observed at the distinct scale $x_0 \sim \log N$ known from the NLIEs for the periodic boundary case. The ratio x_1/x_0 takes large/small values for short/long chains, for which we present explicit solutions derived through iterative numerical methods.

We also explore a scaling limit of the NLIEs, where short-range kernels simplify to delta functions while long-range Cauchy-like elements remain intact. This study establishes a framework for analyzing finite-size corrections and conformal properties of integrable spin chains with non-diagonal boundaries.

Andreas Klümper
Department of Physics, University of Wuppertal, Gaussstraße 20, 42119 Wuppertal, Germany
e-mail: kluemper@uni-wuppertal.de

Xin Zhang
Beijing National Laboratory for Condensed Matter Physics, Institute of Physics, Chinese Academy of Sciences, Beijing 100190, China
e-mail: xinzhang@iphy.ac.cn

1 Introduction

The XXX spin-$\frac{1}{2}$ chain is a prototypical example of quantum integrable systems, renowned for its exact solvability under periodic boundary conditions through Bethe's Ansatz [1]. The foundation of integrability lies in the Yang-Baxter equation [2], a pivotal framework that has driven significant advances in quantum mechanics and statistical physics by enabling the discovery of numerous integrable models. However, the introduction of non-periodic boundary conditions adds complexity, requiring new theoretical tools and methods.

Research on quantum spin systems with non-trivial boundary conditions has a long history. It plays a crucial role in the study of single-impurity systems underlying the Kondo effect [3, 4], which has also inspired investigations into conformal field theories with boundaries [5, 6]. Beyond equilibrium systems with boundaries, spin chains coupled to dissipative boundary baths with controlled polarization have also attracted interest. In such systems, the dynamics become non-unitary, leading to relaxation into a non-equilibrium steady state. At strong dissipation, edge spin fluctuations are suppressed, effectively imposing Dirichlet boundary conditions on the quantum spin chain [7, 8]. Much of the recent research in this area has been driven by theoretical interest. Many studies focus on surface effects of a single impurity, yielding $\mathscr{O}(1)$ corrections to thermodynamic quantities in systems of size N. In this work, we take a step further by examining the mutual correlations of two boundaries at opposite ends of an open Heisenberg chain, where the boundary fields enclose an arbitrary angle. These correlations are of order $\mathscr{O}(1/N)$, revealing novel finite-size effects in boundary-driven quantum spin chains.

The XXX spin-$\frac{1}{2}$ chain with parallel boundary fields was successfully solved using both the coordinate and algebraic Bethe Ansatz [9, 10], and finite-size corrections were subsequently explored in [11]. For more general boundary conditions, Sklyanin's reflection algebra [10, 12] provided a powerful framework to address the factorization of scattering processes at the chain boundaries. This approach culminated in the proof of integrability for the Heisenberg spin chain with non-parallel boundary fields [13].

Non-parallel boundary fields, however, break the $U(1)$ symmetry of the system, presenting challenges for conventional Bethe Ansatz methods. To overcome these obstacles, advanced techniques such as $T-Q$ relations [14, 15], fusion hierarchies [16], and the off-diagonal Bethe Ansatz (ODBA) [17, 18] have been developed. These methods utilize inhomogeneous $T-Q$ relations and hierarchies of transfer matrices, with recent work demonstrating completeness for certain ODBA formulations [19].

Further progress has been achieved through alternative approaches, including the modified algebraic Bethe Ansatz, which utilizes chiral basis states [20–23], the chiral coordinate Bethe ansatz [24] and separation of variables techniques applied to increasingly complex boundary conditions [25–27]. These advancements have expanded the applicability of integrable systems to diverse boundary conditions and physical phenomena.

In [28] physical properties have been calculated that are independent of the angle between the boundary fields, such as the ground-state energy, low-lying excitations and surface terms. In this work, we build on some of the developments to analyze the isotropic Heisenberg chain with arbitrary boundary fields [29] which in turn among other things builds on the inhomogeneous $T-Q$ relation [17, 18]. We here discuss how to use the extended set of NLIEs of [29] to derive data beyond the expressions for the ground-state energy and surface energy. Notably for finite-size corrections, we provide a consistent perspective on deriving $\mathscr{O}(1/N)$ terms in a two step scaling limit.

The structure of the paper is as follows. In Section 2 we give a short review on the NLIEs for the periodic boundary case of the isotropic Heisenberg spin chain. We restrict this to the discussion of the ground state, but present numerical results for various system sizes. In Section 3, we summarize the ODBA approach [17, 18] for the open boundary case with non-parallel boundary fields. We identify an extended set of characteristic "auxiliary functions" that satisfy NLIEs. Section 4 indicates elements of the derivation of these NLIEs and discusses numerical solutions to these. There, qualitatively different features are observed for short and large system sizes. In Section 5, we present the multiplicative scaling limit of the NLIEs and some numerical studies for the simplified, but still non-trivial NLIEs. A conjectural approximate expression for the finite size data of the ground-state energy is given. Finally, conclusions are provided in Section 6.

2 Non-linear integral equations for periodic boundaries

The spin-1/2 Heisenberg model is a well studied quantum system, especially for periodic boundary conditions

$$H_p = \sum_{j=1}^{N} \vec{\sigma}_j \cdot \vec{\sigma}_{j+1}, \qquad \vec{\sigma}_{N+1} := \vec{\sigma}_1 \,. \tag{1}$$

In this paper we are interested in exact integral equations for eigenvalues and their (numerical) solutions. For periodic boundary conditions and arbitrary chain length these were derived in [30, 31] and read for the ground-state of the isotropic system

$$\begin{pmatrix} \log a \\ \log \overline{a} \end{pmatrix} = d + k * \begin{pmatrix} \log A \\ \log \overline{A} \end{pmatrix} . \tag{2}$$

These are non-linear integral equations as the logarithms of a, A, $\overline{a}$, and $\overline{A}$ enter where

$$A(x) := 1 + a(x), \quad \overline{A}(x) := 1 + \overline{a}(x) \,. \tag{3}$$

The functions $a(x)$ and $\overline{a}(x)$ are treated as independent, but "turn out" to be complex conjugate to each other. The integrals are of convolution type. In general the convolution $*$ of two functions f, g is defined by

$$f * g(x) = \frac{1}{2\pi}\int dy f(x-y)g(y). \tag{4}$$

The source (driving) term and the kernel matrix in (2) are

$$d(x) = N\log\tanh\left(\frac{\pi}{4}x\right)\cdot\begin{pmatrix}1\\1\end{pmatrix}, \quad k(x) = \begin{bmatrix}\kappa(x,1) & -\kappa(x-\mathrm{i}\,2^-,1)\\ -\kappa(x+\mathrm{i}\,2^-,1) & \kappa(x,1)\end{bmatrix}, \tag{5}$$

where $2^- = 2-0^+$ and the function κ is related to the digamma function ψ

$$\begin{aligned}\kappa(x,r) := \frac{1}{4}\Big[&\psi\left(\tfrac{1}{4}(r+3+\mathrm{i}x)\right)+\psi\left(\tfrac{1}{4}(r+3-\mathrm{i}x)\right)\\ &-\psi\left(\tfrac{1}{4}(r+1+\mathrm{i}x)\right)-\psi\left(\tfrac{1}{4}(r+1-\mathrm{i}x)\right)\Big].\end{aligned} \tag{6}$$

The ground-state energy is given by a bulk term and a finite size contribution of order $\mathscr{O}(1/N)$ in terms of an integral involving the functions $\log A$ and $\log\overline{A}$

$$E = N(1-4\log 2) - 4\mathrm{i}\left[e' * (\log A + \log\overline{A})\big|_{-\mathrm{i}}\right], \qquad e(x) := \frac{\frac{\pi}{2}}{\cosh\frac{\pi}{2}x}, \tag{7}$$

here written in form of a convolution integral at a specific argument.

In Fig. 1 we show numerical results for chain lengths $N = 10^3, 10^6, 10^9$. The solution functions show a simple qualitative behaviour, $\log A$ is very close to 0 for arguments $|x| < \frac{2}{\pi}\log N$. For $|x| > \frac{2}{\pi}\log N$ the function takes non-zero values with algebraically fast convergence to $\log 2$ for $x\to\infty$. This behaviour is mainly dominated by the source term on the right hand side of (2). The contributions of the convolution integral are of course mostly of quantitative type, new qualitative features are a non vanishing imaginary part for arguments $|x| \simeq \frac{2}{\pi}\log N$ and algebraically decaying asymptotics. Note that similar NLIEs with different driving terms hold for the thermodynamics of the Heisenberg chain and related quantum systems [32–36].

3 Non-parallel boundary fields: eigenvalue equation and characteristic functions

For the spin-1/2 Heisenberg model with isotropic bulk interaction the Hamiltonian of the system with arbitrary boundary fields can be brought to the form

$$H_o = \sum_{j=1}^{N-1}\vec{\sigma}_j\cdot\vec{\sigma}_{j+1} + \frac{1}{p}\sigma_1^z + \frac{1}{q}\left(\sigma_N^z + \xi\sigma_N^x\right), \tag{8}$$

where N is the number of sites, and p, q, and ξ are boundary parameters, where ξ is equal to the tangent of the angle between the boundary fields.

The Hamiltonian is found as member of a family of commuting operators that are generated by an associated family of commuting transfer matrices. We study the

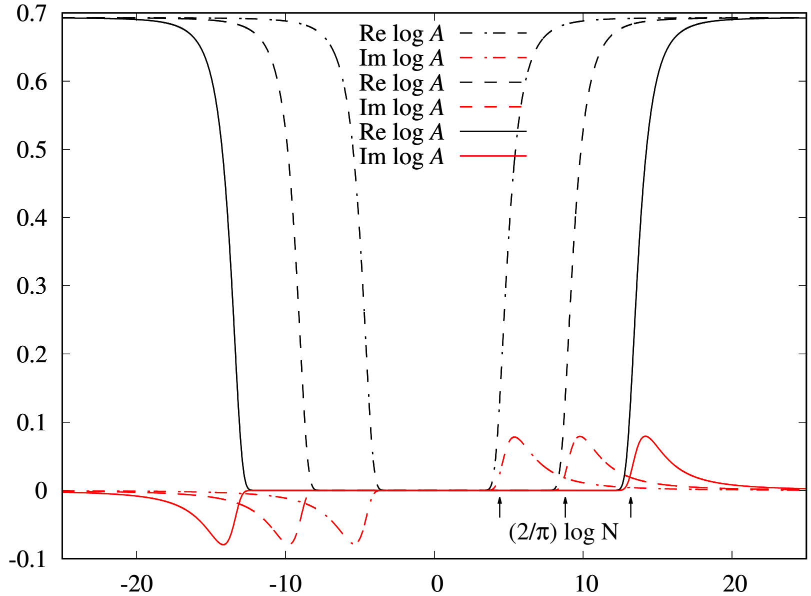

Fig. 1 Graphs of the functions $\log A$ resp. $\mathrm{Re}\log A$ and $\mathrm{Im}\log A$ for the ground-state eigenvalue of the spin-$1/2$ XXX chain with periodic boundary conditions and chain lengths $N = 10^3, 10^6, 10^9$ (dash-dotted, dashed, solid lines). There is one important length scale in the system, $\frac{2}{\pi}\log N$, where at arguments x of this order $\mathrm{Re}\log A(x)$ shows a transition from one flat inner region with values extremely close to 0 to the asymptotic behaviour $\log 2$, and where $\mathrm{Im}\log A(x)$ deviates noticeably from zero.

eigenvalue functions $\Lambda(x)$ for this family of transfer matrices for an even number of sites N. Using the inhomogeneous T-Q relation of [17, 18] with two Q-functions we have

$$\Lambda(x) = \lambda_1(x) + \lambda_2(x) + \lambda_3(x), \tag{9}$$

where we rescaled the function by dropping a constant factor $(\mathrm{i}/2)^{2N+2}$ and we also reparameterized the argument $u = \mathrm{i}x/2 - 1/2$ used in [18] by the new variable x. The summands in (9) are

$$\lambda_1(x) := \phi_1(x)\frac{q_1(x+2\mathrm{i})}{q_2(x)}, \quad \lambda_2(x) := \frac{\phi_2(x)}{q_1(x)q_2(x)}, \quad \lambda_3(x) := \phi_3(x)\frac{q_2(x-2\mathrm{i})}{q_1(x)}, \tag{10}$$

where $q_1(x)$ and $q_2(x)$ are polynomials of degree N with $q_2(x) = q_1(-x)$. The zeros of $q_1(x)$ are called Bethe roots.

The functions $\phi_1(x)$, $\phi_2(x)$, $\phi_3(x)$ are explicitly given by

$$
\begin{aligned}
\phi_1(x) &:= \xi_1 \frac{\varphi(x)}{x}(x-\mathrm{i})^{2N+1}, \qquad \varphi(x) := (x+\mathrm{i}+\mathrm{i}p_1)(x+\mathrm{i}+\mathrm{i}p_2),\\
\phi_2(x) &:= 2\big(1-\xi_1\big)(x^2+1)^{2N+1},\\
\phi_3(x) &:= \xi_1 \frac{\overline{\varphi}(x)}{x}(x+\mathrm{i})^{2N+1}, \qquad \overline{\varphi}(x) := (x-\mathrm{i}-\mathrm{i}p_1)(x-\mathrm{i}-\mathrm{i}p_2),
\end{aligned}
\tag{11}
$$

and we used new combinations of the boundary parameters

$$
\xi_1 := (1+\xi^2)^{1/2}, \qquad p_1 := -2p, \qquad p_2 := -2q/\xi_1. \tag{12}
$$

In [18] the Bethe roots are calculated for relatively short chains by numerically solving for the Bethe equations. These equations are derived from the condition that all potential poles in (9) cancel, resulting in an analytic function $\Lambda(x)$. We do not write down these equations explicitly as we do not use them.

Here we adopt a different resp. opposite approach by using the analyticity of the eigenvalue function directly. For the details we have to refer to [29]. There, three combinations of functions are found to be fundamental to formulating a closed set of integral equations

$$
a(x) := \frac{\lambda_2(x+\mathrm{i})+\lambda_3(x+\mathrm{i})}{\lambda_1(x+\mathrm{i})}, \quad A(x) := 1+a(x) = \frac{\Lambda(x+\mathrm{i})}{\lambda_1(x+\mathrm{i})}, \tag{13}
$$

$$
\overline{a}(x) := \frac{\lambda_1(x-\mathrm{i})+\lambda_2(x-\mathrm{i})}{\lambda_3(x-\mathrm{i})}, \quad \overline{A}(x) := 1+\overline{a}(x) = \frac{\Lambda(x-\mathrm{i})}{\lambda_3(x-\mathrm{i})}, \tag{14}
$$

$$
c(x) := \frac{\lambda_2(x)\Lambda(x)}{\lambda_1(x)\lambda_3(x)}, \qquad C(x) := 1+c(x) = \frac{[\lambda_1(x)+\lambda_2(x)][\lambda_2(x)+\lambda_3(x)]}{\lambda_1(x)\lambda_3(x)}, \tag{15}
$$

with asymptotic behaviour

$$
a(\infty) = \overline{a}(\infty) = 2/\xi_1 - 1, \qquad c(\infty) = 4(1/\xi_1^2 - 1/\xi_1). \tag{16}
$$

A clarification of our terminology is in order. We introduce three functions, two of which share the same notation as those appearing in Sect. 2. However, despite their identical symbols, the functions $a(x)$ and $\bar{a}(x)$ are defined differently here and take different values. Nevertheless, strong similarities exist, the most significant being the (sub-)kernel matrix coupling these functions in the NLIEs (see (5) and (21)). For this reason, we have retained the same notation, trusting that the reader will recognize the distinction when interpreting plots. In particular, we distinguish cases where only $a(x)$ (or equivalently, $\log A$) is shown from those where both $a(x)$ and $c(x)$ (or $\log A$ and $\log C$) appear.

Any energy eigenvalue E of the Hamiltonian is obtained from the logarithmic derivative of the corresponding eigenvalue $\Lambda(x)$ of the transfer matrix. For the ground state eigenvalue with both p and q negative we have, ordered by bulk, surface and finite size terms

$$E = N(1-4\log 2) \tag{17}$$

$$+\pi - 1 - 2\log 2 + \frac{2}{p_1} + \psi\left(\frac{p_1}{4}\right) - \psi\left(\frac{p_1+2}{4}\right) + \frac{2}{p_2} + \psi\left(\frac{p_2}{4}\right) - \psi\left(\frac{p_2+2}{4}\right) \tag{18}$$

$$+4e(x_0) - 2\mathrm{i}\left[e' * (\log A + \log \overline{A})\big|_{-\mathrm{i}}\right]. \tag{19}$$

The last line (19) is a $\mathscr{O}(1/N)$ contribution, because $x_0 \simeq \frac{2}{\pi}\log N$ and the function $\log A + \log \overline{A}$ takes non-negligeable values for arguments only outside the interval $[-x_0, x_0]$. Interestingly, only functions $\log A$ and $\log \overline{A}$ enter the energy formula, but do not satisfy a closed set of integral equations among themselves. Only the set of 3 auxiliary functions (13)-(15) allows for this.

Here, however, we have to skip the derivation of NLIEs for the above defined functions and refer to [29]. That work is considerably involved. Non-technical evidence of this is the qualitatively different behaviour of the functions in comparison to the periodic boundary case as shown in Fig. 2 for relatively short ($N = 10^3$) and Fig. 3 for longeer ($N = 10^6, 10^9$) chains. Here, the functions $\log A$ and $\log \overline{A}$ show non-trivial asymptotics with increase resp. decrease of the imaginary parts by $2\cdot 2\pi\mathrm{i}$. In addition, the set of NLIEs comprises a new third function $C(x) = 1 + c(x)$ with no counter-part in the periodic boundary case.

4 Non-parallel boundary fields case: the non-linear integral equations

The derivation of NLIEs is done in [29] largely following [30, 31, 37, 38] but facing a new challenge that the involved functions show non-vanishing asymptotics. For this, subtraction terms are introduced in the convolution part such that the involved functions show vanishing asymptotics. And for the compensation, counter terms in the driving (source) terms of the NLIEs are used. The subtractions and compensation terms can be chosen to be simply of rational function type with free parameters. The result is

$$\begin{pmatrix} \log a \\ \log \overline{a} \\ \log c \end{pmatrix} = d + K * \begin{pmatrix} \log(A/A(\infty)) - \log\left(\dfrac{x-x_{r+}}{x-x_{r-}} \cdot \dfrac{x-x_{l+}}{x-x_{l-}}\right) \\ \log(\overline{A}/\overline{A}(\infty)) - \log\left(\dfrac{x-x_{r-}}{x-x_{r+}} \cdot \dfrac{x-x_{l-}}{x-x_{l+}}\right) \\ \log(C/C(\infty)) \end{pmatrix}, \tag{20}$$

with kernel matrix

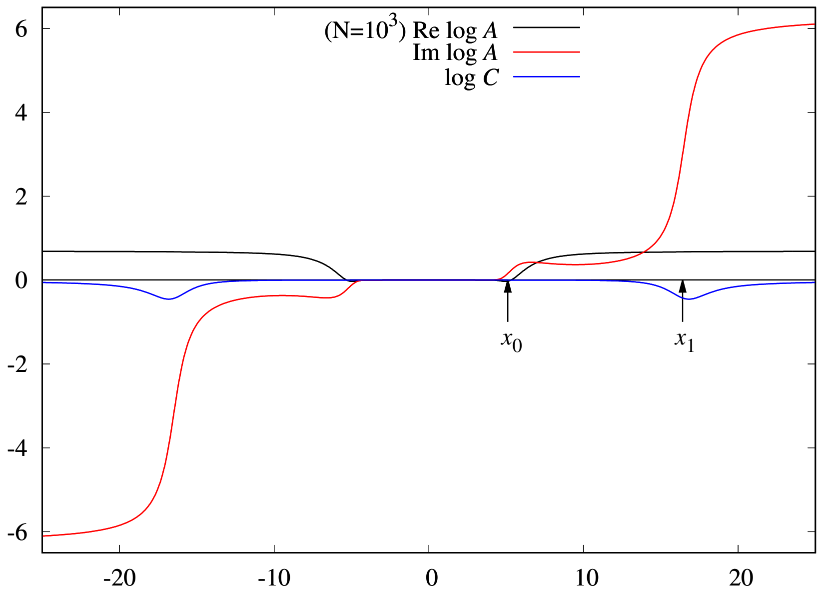

Fig. 2 Graphs of $\log A$ and $\log C$ for the ground-state eigenvalue of the spin-$1/2$ XXX chain with boundary parameters $p=-0.6$, $q=-0.3$, $\xi=0.1$, and system size $N=10^3$. The real (imaginary) part of $\log A$ is even (odd), while $\log C$ is real and even. Two key scales are visible: the zeros $\pm x_0$ of $\log C$, where $x_0 \simeq \frac{2}{\pi}\log N \approx 5.1$. In $[-x_0, x_0]$, $\log C$ remains small and positive, turning noticeably negative outside. Similarly, $\log A$ takes near-zero values in this interval, approaching non-zero asymptotics outside. At $x_1 \sim 16.5$ $(> x_0)$ and at $-x_1$, $\log C$ has minima, while the imaginary part of $\log A$ shows a steady increase, ultimately reaching $+2\pi$ as $x \to +\infty$.

$$K(x) = \begin{bmatrix} \kappa(x,1) & -\kappa(x-\mathrm{i}2^-,1) & -\mathrm{i}/(x-\mathrm{i}) \\ -\kappa(x+\mathrm{i}2^-,1) & \kappa(x,1) & \mathrm{i}/(x+\mathrm{i}) \\ \mathrm{i}/(x+\mathrm{i}) & -\mathrm{i}/(x-\mathrm{i}) & 0 \end{bmatrix}, \tag{21}$$

where the function κ is the same as already given above in (6). Note that the logarithms of analytic functions as appearing above are analytic functions themselves without any $\pm 2\pi\mathrm{i}$ jumps.

Note that the careful prescription for the convolution integrals is necessary because of the slow asymptotics of K_{31} and K_{32} and the curious property that the functions $\log A$ and $\log \overline{A}$ show non-trivial windings, see Fig. 2 for a system with size $N=10^3$, still to be considered small on grounds that become clearer shortly. The equations (20) are non-linear integral equations (NLIEs) for the functions a, $\overline{a}$, c, because $A=1+a$, $\overline{A}=1+\overline{a}$, $C=1+c$. Numerical solutions are obtained by iterative treatments and evaluations of the convolution integrals by the Fast Fourier Transform. In parallel, the zeros $\pm x_0$ of $\Lambda(x)$ are determined by solving $a(x_0+\mathrm{i})=-1$, evaluating the right-hand sides of the integral equations off the real axis. The value of x_0 is iteratively updated during the numerical treatment. This parameter also appears in the source term (24) but has no counterpart in the case of periodic boundary conditions, where the ground-state eigenvalue function – not discussed in Sect. 2 – has no real-axis zeros.

In the counter terms x_{r+} and x_{r-} are complex numbers with positive real part and positive resp. negative imaginary parts. And x_{l+} and x_{l-} are defined similarly with negative real parts. The introduced functions subtract the winding behaviour observed in the functions $\log A$ and $\log\overline{A}$. Now the inhomogeneity d is a tuple of three functions containing the counter terms

$$\begin{aligned} d_1(x) &= (2N+1)\log\tanh\left(\frac{\pi}{4}x\right) + \frac{\pi}{2}\mathrm{i} - \mathrm{i}\alpha(x-\mathrm{i},1) \\ &\quad + \mathrm{i}\alpha(x-\mathrm{i},p_1) + \mathrm{i}\alpha(x-\mathrm{i},p_2) - \mathrm{i}\alpha(x-x_0-\mathrm{i},1) - \mathrm{i}\alpha(x+x_0-\mathrm{i},1) \\ &\quad + \log\left(a(\infty)\cdot\frac{x-x_{r+}-2\mathrm{i}}{x-x_{r-}}\cdot\frac{x-x_{l+}-2\mathrm{i}}{x-x_{l-}}\right), \end{aligned} \tag{22}$$

$$\begin{aligned} d_2(x) &= (2N+1)\log\tanh\left(\frac{\pi}{4}x\right) - \frac{\pi}{2}\mathrm{i} + \mathrm{i}\alpha(x+\mathrm{i},1) \\ &\quad - \mathrm{i}\alpha(x+\mathrm{i},p_1) - \mathrm{i}\alpha(x+\mathrm{i},p_2) + \mathrm{i}\alpha(x-x_0+\mathrm{i},1) + \mathrm{i}\alpha(x+x_0+\mathrm{i},1) \\ &\quad + \log\left(\overline{a}(\infty)\cdot\frac{x-x_{r-}+2\mathrm{i}}{x-x_{r+}}\cdot\frac{x-x_{l-}+2\mathrm{i}}{x-x_{l+}}\right), \end{aligned} \tag{23}$$

$$d_3(x) = \log\left(c(\infty)\cdot\frac{x^2(x^2-x_0^2)}{(x-x_{r-}+\mathrm{i})(x-x_{r+}-\mathrm{i})(x-x_{l-}+\mathrm{i})(x-x_{l+}-\mathrm{i})}\right). \tag{24}$$

Here $\alpha(x,r)$ is the integral of the function $\kappa(x,r)$ with respect to x

$$\alpha(x,r) := \mathrm{i}\log\frac{\Gamma\left(\frac{1}{4}(r+3-\mathrm{i}x)\right)\Gamma\left(\frac{1}{4}(r+1+\mathrm{i}x)\right)}{\Gamma\left(\frac{1}{4}(r+3+\mathrm{i}x)\right)\Gamma\left(\frac{1}{4}(r+1-\mathrm{i}x)\right)}. \tag{25}$$

Note that the functions $\kappa(x,r)$ and $\alpha(x,r)$ are real valued for real arguments x, r.

The concrete values of $x_{r\pm}$ and $x_{l\pm}$ drop out of the calculations and affect at best the accuracy of the calculations. For practical purposes we choose for these numbers

$$x_{r\pm} = \tilde{x}_1 \pm \mathrm{i}\,\delta, \qquad x_{l\pm} = -\tilde{x}_1 \pm \mathrm{i}\,\delta, \tag{26}$$

with some $\delta > 0$ and $\tilde{x}_1$ is an estimate of the location of the transition of the imaginary part of $\log A$ from small resp. practically zero values to $+2\pi$ as explained in Fig. 2. The *optimal* choice of the parameters $\tilde{x}_1$ and δ for the discussed counterterms ensures the fastest convergence of the iterative numerical treatment and provides the *best* estimate for the location x_1 of the transition in the imaginary part of $\log A$. Unlike the zero x_0 of the eigenvalue function $\Lambda(x)$, the parameter x_1 is not precisely defined. However, the transition in $\mathrm{Im}\log A$ arises from a well-defined complex conjugate pole-zero pair of $A(x)$. Here, we do not analyze these structures in detail, as their precise properties are irrelevant for calculating the energy which only depends on the real part of $\log A$ (19) which does not have any remarkable structure at x_1.

A practical approach for iterating the NLIEs is to use initial data resembling solutions of the Bethe ansatz equations, feasible for small system sizes ($N \sim 10$). For such systems, $a(x)$ remains near zero for x close to 0 but grows in magnitude for $|x|$ beyond $\frac{2}{\pi}\log N$, eventually with $a(x)$ encircling -1 counter-clockwise at some x_1, causing a sharp increase in $\mathrm{Im}\log A$, see Fig. 2. This behavior is critical for understanding the winding in $\log A$.

Convergence of the NLIEs was achieved for "short chains" (like $N = 10^3$ for $\xi = 0.1$), but increasing N "soon" results in the divergence of the iterations, independent of boundary parameters. We found that x_0, the zero of $c(x)$, always scales as $\frac{2}{\pi}\log N$, separating regions where $a(x)$ is near zero from those where it becomes order 1. For short chains, the position x_1 of the winding observed in $\log A$ satisfies $x_1 \gg x_0$, but increasing N leads to $x_1 \sim x_0$.

For large sizes, no initial data reliably captured the winding at $x_1 > x_0$. Surprisingly, the winding occurs in the "forbidden region" $[-x_0, x_0]$, where $a(x)$ is nearly zero. For large sizes, initial data with winding at $x_1 < x_0$ lead to convergence, see Fig. 3. For all systems, zeros of $q_1(x)$ and $q_2(x)$ form a pole-zero pair of $A(x)$, causing $A(x)$ taking a loop around 0. Tracking this pair as N increases shows it moving away from the origin initially but eventually stabilizing at a finite distance and moving back at very large N.

The condition for this to occur is that the separation between the zero and pole in the pair approaches zero exponentially fast. Under this condition, the aforementioned winding happens so rapidly that the convolution integrals generate contributions canceling the leading term, $(2N+1)\log\tanh\frac{\pi}{4}x$. Based on this reasoning, we successfully found solutions to the NLIEs for significantly larger system sizes, as illustrated in Fig. 3.

5 The two step scaling limit

In the periodic boundary case the finite size data of order $\mathscr{O}(1/N)$ are obtained in an *additive scaling limit* [31] of the NLIEs (2) for the $N \to \infty$ limits of the functions with shifted argument, e.g. for the "right movers"

$$a_r(x) := \lim_{N\to\infty} a\left(x + \tfrac{2}{\pi}\log N\right), \quad \text{and} \quad \overline{a}_r(x) := \lim_{N\to\infty} \overline{a}\left(x + \tfrac{2}{\pi}\log N\right), \tag{27}$$

and similar for functions obtained with a shift $x \to x - \frac{2}{\pi}\log N$ describing "left movers". These functions satisfy sets of NLIEs very similar to (2), however with source terms $-2\exp(-x)$. A similar scaling limit has to be considered here for the derivation of the finite size corrections. However, a direct application of the above strategy does not yield a closed set of NLIEs just among the "right movers" or among the "left movers". This happens because we have long ranged kernel elements that couple "right movers" and "left movers".

The scaling limit consists of two steps. In the first step we formulate a *multiplicative scaling limit* for all three functions (here we are allowed to use $x_0 = \frac{2}{\pi}\log N$ as

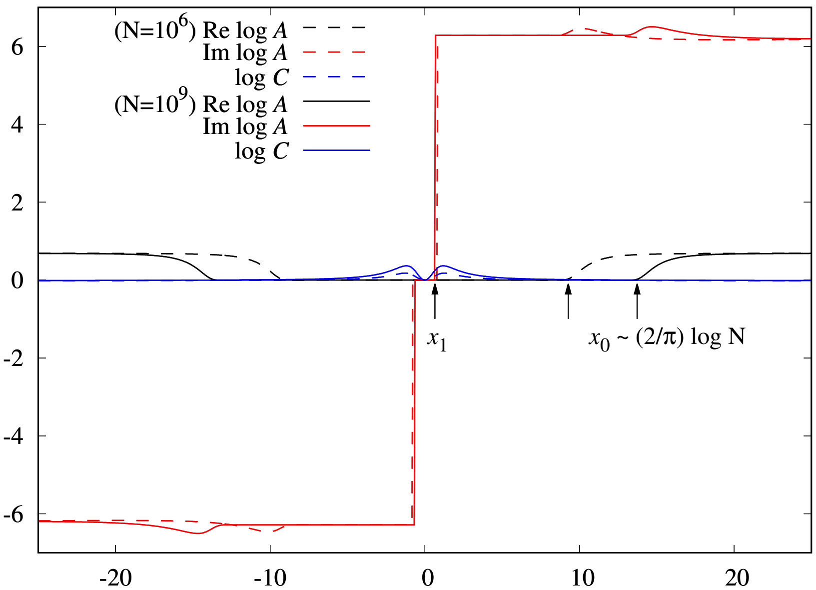

Fig. 3 Plot of $\log A$ and $\log C$ for the ground-state eigenvalue of the spin-$1/2$ XXX chain, with parameters as in Fig. 2, for $N = 10^6$ (dashed) and $N = 10^9$ (solid). The zeros of $\log C$ are at $\pm x_0$, with $x_0 = 9.27..\ (13.72..) \simeq \frac{2}{\pi}\log N$ for $N = 10^6\ (10^9)$. Unlike Fig. 2, the point x_1, where $\mathrm{Im}\log A$ jumps sharply from 0 to 2π, satisfies $x_1 < x_0$ and appears step-like. Here, $x_1 = 0.78..\ (0.64..)$ for $N = 10^6\ (10^9)$, showing that x_0 increases and x_1 decreases with N. Within $[-x_0, x_0]$, $\log C$ is positive and large, while outside it is flat and negative. Here *maxima* in $\log C$ align with the transitions of $\mathrm{Im}\log A$ at $\pm x_1$. Note that in the case of shorter chains, *minima* in $\log C$ appeared, see Fig. 2.

identity)

$$a_m(x) := \lim_{N\to\infty} a(x_0 \cdot x)\,, \quad \overline{a}_m(x) := \lim_{N\to\infty} \overline{a}(x_0 \cdot x)\,, \quad c_m(x) := \lim_{N\to\infty} c(x_0 \cdot x)\,, \tag{28}$$

which leads to a well-defined set of NLIEs for all three functions.

We impose that the kinks do not increase with system size, actually their values appear to shrink to the origin. Certainly in the multiplicative scaling limit the kink positions take the value 0 and many other functions in the source terms simplify drastically resulting in the following NLIEs

$$\log a_m(x) = \log a(\infty) + \frac{1}{2}\log\frac{A_m(x)}{\overline{A}_m(x)} - \frac{\mathrm{i}}{x - \mathrm{i}\varepsilon} * \log\frac{C_m}{C(\infty)}, \quad \text{for } x \notin [-1,1]\,,$$
$$\text{else } a_m(x) = 0, \tag{29}$$

$$\log c_m(x) = \log\left(c(\infty)\cdot\frac{x^2-1}{x^2}\right) + \frac{\mathrm{i}}{x+\mathrm{i}\varepsilon} * \log\frac{A_m}{A(\infty)} - \frac{\mathrm{i}}{x-\mathrm{i}\varepsilon} * \log\frac{\overline{A}_m}{\overline{A}(\infty)}\,, \tag{30}$$

where $a(\infty)$ is the limit of the function $a(x)$ for $x \to \infty$, etc. In the derivation of (30) from (20) we used the limiting functions (28) with an additional simplification for their logarithms. The counter terms in (20) and (22,23), i.e. the rational functions with parameters $x_{r,\pm}$ and $x_{l,\pm}$, take the limits 1. The logarithms, however, of these functions are step functions that take values $\pm 2\pi\mathrm{i}$. Absorbing these constants into the functions $\log A_m$ and $\log \overline{A}_m$ leads to logarithms of A_m and $\overline{A}_m$ on the standard branch. The counter terms in (24) appearing in the denominator simplify to a x^4 such that the second equation in (30) results implying a pole of second order at $x = 0$ for the function $c_m(x)$. Numerical results for (29) and (30) are shown in Fig. 4.

In the second step, but not treated here, we consider the *additive scaling limit* of just the two functions a and $\overline{a}$ and take as input for the function c the data of c_m obtained in the *multiplicative scaling limit*.

Finally we give results for the finite size term of the ground-state energy for a system with angle ϕ between the boundary fields, i.e. $\xi = \tan\phi$ and v being the velocity of elementary excitations

$$E_N - Ne_0 - f_s = -\frac{\pi v}{24N}\left(1 - 6\left(1 - \frac{\phi}{\pi}\right)^2\right),$$

where e_0 is the ground state energy per site (17) and f_s the surface energy (18). This result is still of conjectural nature based on small ϕ data.

6 Conclusion

The XXX spin chain with non-diagonal boundary fields remains a central but challenging model in the study of quantum integrable systems with non-trivial boundaries [13–23, 25–28]. Despite its significance, finding an exact solution has been a longstanding challenge. Significant progress has been achieved through the development of inhomogeneous $T-Q$ relations and the off-diagonal Bethe Ansatz (ODBA) [17, 18] . These advances, along with subsequent extensions [19–23, 25–27], have paved the way for deeper investigations into the model's structure.

In this work, we explored exact non-linear integral equations (NLIEs) for three auxiliary functions derived in [29]. A major contribution is the introduction of the function $c(x)$, which incorporates the inhomogeneous term of the $T-Q$ relation, complementing the classical functions $a(x)$ and $\overline{a}(x)$. This framework captures essential phenomena such as the winding behavior, where $\log A(x)$ and $\log \overline{A}(x)$ exhibit steep increases by $2\pi\mathrm{i}$ at a characteristic scale x_1. Additionally, the function $\log C(x)$ becomes zero at a separate scale x_0. Importantly, our analysis revealed that x_1 and x_0 are independent, with their ratio x_1/x_0 being large for short chains and small for long chains. Numerical results validated these findings for both regimes.

The large-N results facilitated the formulation of a two-step scaling limit for the NLIEs. In the first step, we introduced a multiplicative scaling limit, in which the non-trivial long-range kernel elements are preserved. Unlike the periodic boundary

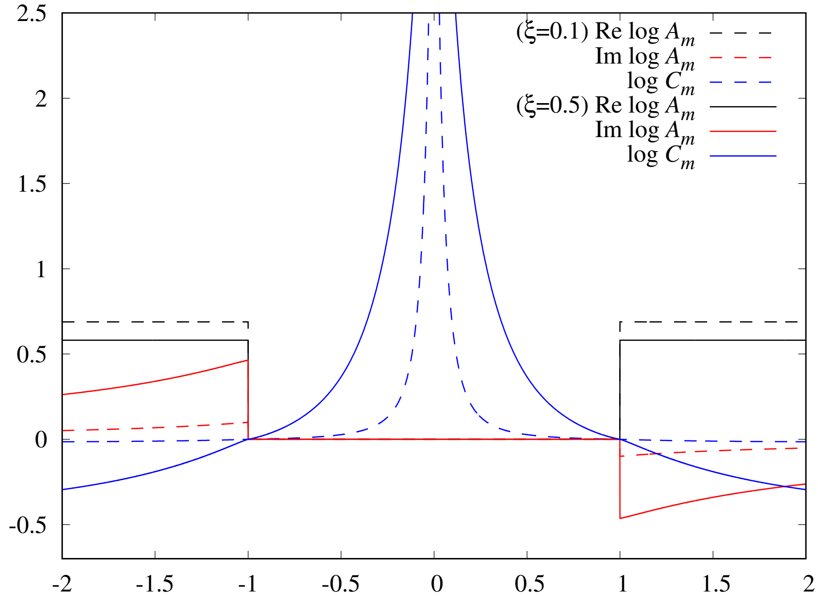

Fig. 4 Plot of the functions $\log A_m$ and $\log C_m$ defined in the multiplicative scaling limit and satisfying the NLIEs (30). The functions depend only on the parameter ξ. Here we show results for two cases, $\xi = 0.1$ and $\xi = 0.5$.

case, where solutions simplify to piecewise constant functions, the open boundary case retains a rich structure of non-trivial solutions. Based on these results, we conjectured a formula for the finite-size corrections to the ground-state energy. The second, additive scaling limit, which finalizes this analysis, will be detailed in future work.

Acknowledgements X.Z. acknowledges financial support from the Alexander von Humboldt Foundation. A.K. acknowledges financial support by Deutsche Forschungsgemeinschaft through FOR 2316 and hospitality by the Innovation Academy for Precision Measurement Science and Technology, Wuhan, A.K.'s work has been funded by the Chinese Academy of Sciences President's International Fellowship Initiative, Grant No. 2024PVA0036.

References

1. H. Bethe, *Zur Theorie der Metalle. I. Eigenwerte und Eigenfunktionen der linearen Atomkette.*, Z. Physik **71** (1931), no. 3/4, 205–26.
2. R. J. Baxter, *Exactly solved models in statistical mechanics*, Academic Press, 1982.
3. N. Andrei, *Diagonalization of the Kondo Hamiltonian*, Phys. Rev. Lett. 45.5 (1980): 379.

4. P. B. Wiegmann, *Exact solution of the sd exchange model (Kondo problem)*, J. Phys. C: Solid State Physics 14.10 (1981): 1463.
5. J. L. Cardy, *Conformal invariance and surface critical behavior*, Nucl. Phys. B 240.4 (1984): 514-532.
6. I. Affleck, and A. W. W. Ludwig, *Exact critical theory of the two-impurity Kondo model*, Phys. Rev. Lett. 68.7 (1992): 1046.
7. P. Zanardi and L. C. Venuti, *Coherent quantum dynamics in steady-state manifolds of strongly dissipative systems*, Phys. Rev. Lett. 113, 240406 (2014).
8. V. Popkov, S. Essink, C. Presilla, and G. M. Schütz, *Effective quantum Zeno dynamics in dissipative quantum systems*, Phys. Rev. A 98, 052110 (2018).
9. F. C. Alcaraz, M. N. Barber, M. T. Batchelor, R. Baxter, and G. Quispel, *Surface exponents of the quantum XXZ, Ashkin-Teller and Potts models*, J. Phys. A: Math. Gen. **20** (1987), 6397.
10. E. K. Sklyanin, *Boundary conditions for integrable quantum systems*, J. Phys. A: Math. Gen. **21** (1988), 2375.
11. H. Asakawa and M. Suzuki, *Finite-size corrections in the XXZ model and the Hubbard model with boundary fields*, Journal of Physics A: Mathematical and General **29** (1996), 225.
12. I. V. Cherednik, *Factorizing particles on a half-line and root systems*, Theor. Math. Phys. **61** (1984), 977–983.
13. H. De Vega and A. González-Ruiz, *Boundary K-matrices for the XYZ, XXZ and XXX spin chains*, J. Phys. A: Math. Gen. **27** (1994), 6129.
14. R.I. Nepomechie, *Solving the open XXZ spin chain with nondiagonal boundary terms at roots of unity*, Nucl. Phys. B **622** (2002), 615.
15. R.I. Nepomechie, *Functional relations and Bethe ansatz for the XXZ chain*, J. Stat. Phys. **111** (2003), 1363.
16. H. Frahm, J. H. Grelik, A. Seel, and T. Wirth, *Functional Bethe ansatz methods for the open XXX chain*, J. Phys. A **44** (2011), 015001.
17. J. Cao, W.-L. Yang, K. Shi, and Y. Wang, *Off-diagonal Bethe ansatz solutions of the anisotropic spin-1/2 chains with arbitrary boundary fields*, Nucl. Phys. B **877** (2013), 152–175.
18. Y. Wang, W.-L. Yang, J. Cao, and K. Shi, *Off-diagonal Bethe ansatz for exactly solvable models*, Springer, 2016.
19. R. I. Nepomechie, *An inhomogeneous T-Q equation for the open XXX chain with general boundary terms: completeness and arbitrary spin*, Journal of Physics A: Mathematical and Theoretical **46** (2013), no. 44, 442002.
20. S. Belliard, *Modified algebraic Bethe ansatz for XXZ chain on the segment – I: Triangular cases*, Nuclear Physics B **892** (2015), 1–20.
21. S. Belliard and R. A. Pimenta, *Modified algebraic Bethe ansatz for XXZ chain on the segment – II: General cases*, Nuclear Physics B **894** (2015), 527–552.
22. N. Crampe, *Algebraic Bethe ansatz for the XXZ Gaudin models with generic boundary*, SIGMA **13** (2017), 094.
23. J. Avan, S. Belliard, N. Grosjean, and R.A. Pimenta, *Modified algebraic Bethe ansatz for XXZ chain on the segment – III – proof*, Nuclear Physics B **899** (2015), 229–246.
24. X. Zhang, A. Klümper, and V. Popkov, *Chiral coordinate Bethe ansatz for phantom eigenstates in the open XXZ spin-1/2 chain*, Physical Review B **104** (2021), 195409.
25. H. Frahm, A. Seel, and T. Wirth, *Separation of Variables in the open XXX chain*, Nucl. Phys. B **802** (2008), 351–367.
26. G. Niccoli, *Non-diagonal open spin-1/2 XXZ quantum chains by separation of variables: complete spectrum and matrix elements of some quasi-local operators*, Journal of Statistical Mechanics: Theory and Experiment **2012** (2012), P10025.
27. S. Faldella, N. Kitanine, and G. Niccoli, *The complete spectrum and scalar products for the open spin-1/2 XXZ quantum chains with non-diagonal boundary terms*, Journal of Statistical Mechanics: Theory and Experiment **2014** (2014), P01011.
28. J.-S. Dong, P. Lu, P. Sun, Y. Qiao, J. Cao, K. Hao, and W.-L. Yang, *Exact surface energy and elementary excitations of the XXX spin-1/2 chain with arbitrary non-diagonal boundary fields*, Chinese Physics B **32** (2023), 017501.

29. Holger Frahm, Andreas Klümper, Dennis Wagner, and Xin Zhang, *Non-linear integral equations for the XXX spin-1/2 quantum chain with non-diagonal boundary fields*, arXiv:2502.07229
30. A. Klümper and M. T. Batchelor, *An analytic treatment of finite-size corrections of the spin-1 antiferromagnetic XXZ chain*, J. Phys. A **23** (1990), no. 5, L189–95.
31. Andreas Klümper, Murray T. Batchelor, and Paul A. Pearce, *Central charges of the 6- and 19-vertex models with twisted boundary conditions*, J. Phys. A **24** (1991), no. 13, 3111–33.
32. A. Klümper, *Free energy and correlation length of quantum chains related to restricted solid-on-solid lattice models*, Ann. Physik **1** (1992), 540.
33. C. Destri and H. J. de Vega, *New thermodynamic Bethe ansatz equations without strings*, Phys. Rev. Lett. **69** (1992), 2313.
34. A. Klümper, *Thermodynamics of the anisotropic spin-1/2 Heisenberg chain and related quantum chains*, Z. Phys. B **91** (1993), 507.
35. C. Destri and H. J. de Vega, *Unified approach to thermodynamic Bethe ansatz and finite size corrections for lattice models and field theories*, Nucl. Phys. B **438 [FS]** (1995), 413.
36. J. Suzuki, *Spinons in magnetic chains of arbitrary spins at finite temperatures*, J. Phys. A **32** (1999), 2341.
37. G. Jüttner and A. Klümper, *Exact calculation of thermodynamical quantities of the integrable $t-J$ model*, Europhys. Lett. **37** (1997), no. 5, 335–340.
38. G. Jüttner, A. Klümper, and J. Suzuki, *Exact thermodynamics and Luttinger liquid properties of the integrable $t-J$ model*, Nucl. Phys. B **487** (1997), no. 3, 650–674.